

## **TRANSMITTER AND RECEIVER DESIGN OF AN EXPERIMENTAL AIRBORNE SYNTHETIC APERTURE RADAR SENSOR**

**Y. K. Chan, B. K. Chung, and H. T. Chuah**

Faculty of Engineering, Multimedia University  
63100 Cyberjaya, Malaysia

**Abstract**—An Experimental Airborne Synthetic Aperture Radar (SAR) Sensor has been designed and developed at Multimedia University, Malaysia. The airborne system is an inexpensive C-band, single polarization, linear-FM airborne radar sensor. An innovative cancellation network is implemented to overcome the poor isolation of the circulator thus allow a single antenna to be used for transmitting and receiving the radar signal. The system will be used for monitoring and management of earth resources such as paddy fields, oil palm plantation and soil surface. This paper highlights the design and development of the SAR transmitter and receiver, as well as the evaluation result of the sensor. Calibration has been performed in the laboratory to verify the performance of the radar sensor. External calibration is accomplished by using three artificial point targets, i.e., 12" conducting sphere, 4" × 8" dihedral corner reflector and 8" trihedral corner reflector. The field measurements are conducted in an empty car park, which is a low reflection outdoor environment. Both range detection and radar cross section (RCS) measurement capability are verified in the field experiments.

### **1 Introduction**

### **2 System Descriptions**

#### 2.1 Transmitter

#### 2.2 Receiver

### **3 Calibration and Verification**

#### 3.1 Subsystem Performance Test, RF Feedback Calibration and Internal Calibration

#### 3.2 Field Measurement

## 4 Conclusion

### References

#### 1. INTRODUCTION

Since World War II, radar technology has advanced into the spectrum of millimeter and micrometer wavelengths. The application of radar equipment is no longer confined to looking up at aircraft or looking out at ships. Airborne and spaceborne radars, capable of producing images of ground, have been developed and extensively used in remote sensing applications. In the 1950s, Real Aperture Imaging Radar (or Side Looking Airborne Radar, SLAR) was developed to produce better quality images for military use. Optical image processing techniques were used both to create imagery and for analysis. Large antenna that produces narrow radiation beamwidth must be used for scanning of the earth terrain in order to achieve the required resolution. However, the image formed by SLAR is poor in azimuth resolution. In order to obtain high-resolution image one has to resort either to an impractically long antenna or to employ wavelengths so short that the radar must contend with severe attenuation in the atmosphere. In airborne application particularly the antenna size and weight are restricted.

The recent development in Synthetic Aperture Radar (SAR) technology has made possible a much higher resolution to be achieved using a small antenna. SAR is a technique which uses signal processing to improve the resolution beyond the limitation of physical antenna aperture [1]. In SAR, forward motion of actual antenna is used to 'synthesize' a very long antenna. SAR allows the possibility of using longer wavelengths and still achieving good resolution with antenna structures of reasonable size.

SAR has been shown to be very useful over a wide range of applications, including high resolution geological and topological mapping, sea and ice monitoring [2], military surveillance, mining [3], hydrology, oil pollution monitoring [4], oceanography [5] etc. The potential of SAR in a diverse range of application led to the development of a number of airborne and spaceborne SAR systems.

The use of SAR for remote sensing is particularly suited for tropical country such as Malaysia. By proper selection of operating frequency, the microwave signal can penetrate clouds, haze, rain precipitation with very little attenuation, thus allowing operation in unfavorable weather condition that preclude the use of visible-light/infrared system [6]. Since SAR is an active sensor, which provides its

own source of illumination, it can therefore operate day and night, illuminate the earth surface at variable look angle, and wide area coverage can be selected. In addition, the topography change can be derived from phase difference between measurement using radar interferometry. For national monitoring and management of earth resources, limited number and untimely supply of the required SAR images have been a major problem. Therefore the need for developing our own SAR technology and sensor system is apparent.

A SAR system has been developed at Faculty of Engineering, Multimedia University. It will serve as a test-bed for demonstrating SAR technology and acquiring data for the development of radar processing techniques and applications. The proposed system is an airborne, C-band, single polarization, linear-FM SAR. The construction and testing of the SAR sensor prototype was completed in early 2002. A series of indoor and outdoor experiments has been conducted to verify the capability of the radar sensor.

**Table 1.** System level requirements.

Operating frequency	6 GHz (5 cm)
Polarization	VV, single polarization
Modes of operation	Stripmap
Waveform type	Linear FM
Incident angle	50°
Target types	Distributed targets with $\sigma^\circ$ between 0 dB and -30 dB
Spatial resolution	10 m (azimuth), 10 m (range)
Swath width	10 km
Altitude	~ 7.5 km
Azimuth 3-dB bandwidth	3°
Elevation pattern width	24°
Operating platform	Airborne
Platform speed	100 m/s

Table 1 summarizes the system-level requirements. The center frequency of our system is selected at C-band (6 GHz). We use single polarization mode for target classification and multi-temporal change detection. VV-polarization (Vertical transmit/Vertical receive polarization) is the preferred configuration since it is sensitive to

the vegetation's vertical canopy structure, and thus providing the opportunity for crop type and growth stage discrimination. The system will operate in stripmap mode with incidence angle of 50 degree (swath width = 10 km). It can produce SAR imagery of all classes of terrain with scattering coefficient,  $\sigma^{\circ}$ , between 0 and  $-30$  dB. The spatial resolution is  $10\text{ m} \times 10\text{ m}$ . In order to obtain reliable and accurate data, the airborne SAR platform should maintain a constant-velocity straight-and-level flight. Preferably, the aircraft flies at an altitude of 7500 m above sea level to avoid the low altitude turbulence in the troposphere.

## 2. SYSTEM DESCRIPTIONS

The radar hardware can be functionally divided into three assemblies: (i) Transmitter; (ii) Receiver; and (iii) Antenna. Connectorized coaxial hardware implementation approach is employed in our design. The advantages of this approach are lower cost, fastest development and convenient for testing and troubleshooting. It is also easy to be modified when improvement is required. Most of the RF components are selected with SMA connector. Semi-rigid and flexible coaxial cables are used for interconnecting between components.

### 2.1. Transmitter

Fig. 1 shows the block diagram of the airborne SAR sensor. Basically it can be sub-divided into two subsections: the transmitter and the receiver. The main functions of the transmitter are to generate the desired waveform, amplify it and transmit via an antenna. The transmitter consists of an exciter, a high power amplifier (HPA), a stable local oscillator (STALO), a modulation circuitry, a chirp mode gate and some RF accessories such as RF cables and isolators. The coherent radar signal originates in the STALO. 10 MHz STALO is used as reference signal for chirp generator and other local oscillator (LO) to maintain the coherence of SAR system. The modulation circuit provides proper pulse modulation (PM) and frequency modulation (FM) signal to the chirp mode gate and the exciter. The exciter generates the desired LFM waveform (6 GHz center frequency with 20 MHz bandwidth). Using a directional coupler, a small fraction of the chirp signal is coupled to the quadrature mixer in the receiver to act as reference signal. Major portion of the signal is routed to a solid state high power amplifier with 40-dB gain. The amplified signal is then radiated through the antenna via a circulator.

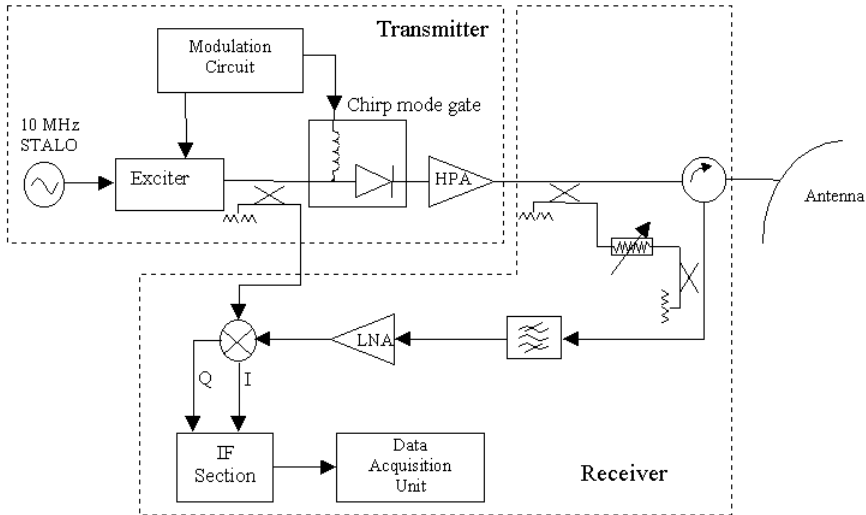


**Figure 1.** Component level diagram of the C-band SAR transmitter and receiver.

## 2.2. Receiver

The function of a radar receiver is to amplify the echoes of the radar transmission and to filter them in a manner that will provide the maximum discrimination between desired echoes (ground) and undesired interference. The front-end circuitry of the receiver selects the input frequency band and amplifies the incoming signal to a proper level for the detector and subsequent low frequency circuitry. It consists of a low noise amplifier (LNA), a band pass filter, a quadrature mixer and a cancellation network (CN).

A cancellation network is introduced to prevent the saturation of the receiver due to poor isolation of the circulator. Fig. 2 shows the conventional circulator and component level diagram of the cancellation network. It consists of 2 directional couplers (C1 and C2) and a 20 dB variable attenuator (R1). The length of coaxial cables for making the interconnection has been properly selected for optimum performance.

Conventional single antenna configuration uses a circulator to transmit and receive the signal via an antenna. The main problem is the isolation of circulator is poor. The leakage signal will give rise to poor signal-to-interference ratio and saturation of receiver amplifier. Fig. 3 shows the  $S_{21}$  of the circulator. It is possible to remove the

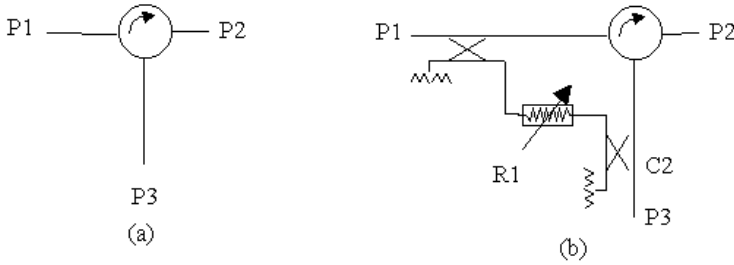


**Figure 2.** Component level diagram of a) Single circulator b) Cancellation network.

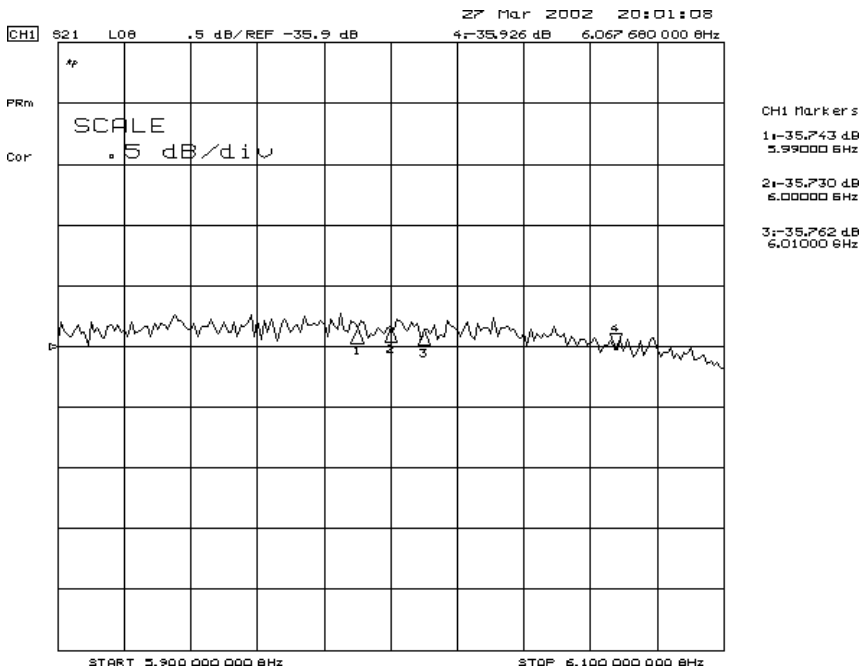


**Figure 3.**  $S_{21}$  of single circulator.

leakage signal from receiver by injecting a sample of the signal in equal amplitude but opposite phase into the receiver circuit. The leakage signal can be measured by terminating both directional couplers with  $50\ \Omega$  load. The measurement setup is shown in Fig. 4. Both the phase and amplitude of  $S_{21}$  are measured across the operating bandwidth of our SAR system.

The sample of source signal is coupled from main line by the first

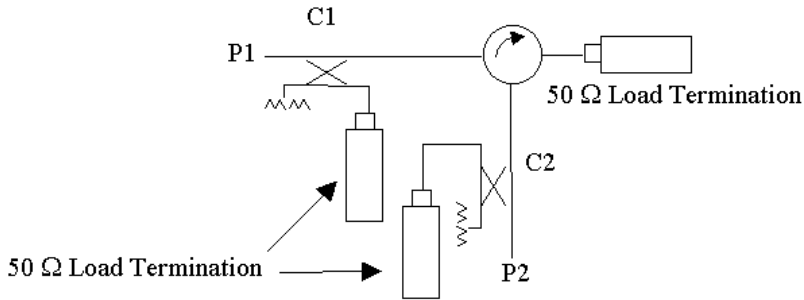


**Figure 4.**  $S_{21}$  measurement setup of leakage signal.

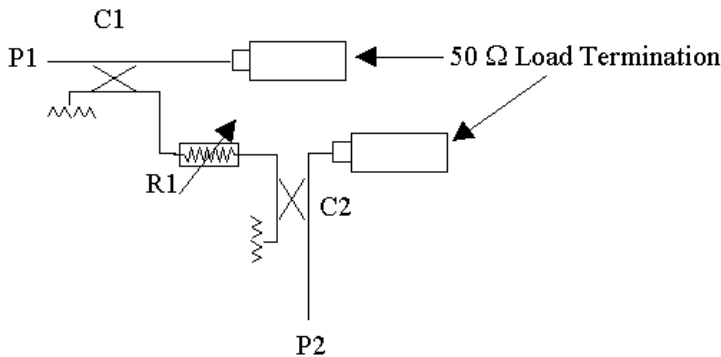


**Figure 5.**  $S_{21}$  measurement setup of coupled signal.

directional coupler, C1 and injected into receiver by second directional coupler, C2. The length of the RF cables is calculated and the variable attenuator, R1 is adjusted such that the coupled signals have the same magnitude as the leakage signal but  $180^\circ$  out of phase. These signals are measured using the setup shown in Fig. 5. Finally  $S_{21}$  of the cancellation network is measured and an excellent isolation of more than  $-62$  dB can be achieved. The result is shown in Fig. 6.

A low noise amplifier (LNA) with a noise figure of 1.6 dB and a band pass filter are placed at the front end of the receiver. The LNA amplifies the received echo from the antenna by 30 dB and improves the sensitivity of the system. A combline band-pass filter is inserted at the receiver to reject any unwanted signal outside the passband. This signal is then down-converted to IF by a quadrature mixer and produces full-phase IF signals ( $I$  and  $Q$ ). A high-speed analog-to-digital converter (ADC) is used to digitize the down-converted signal to data stream and stored in a high-density digital recorder (HDDR).

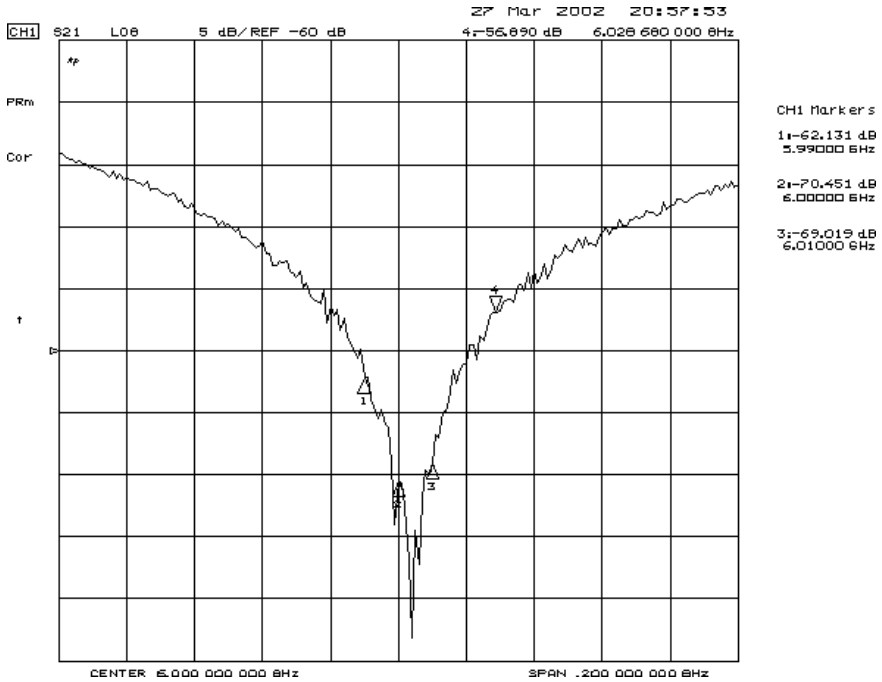


**Figure 6.**  $S_{21}$  of cancellation network.

The main functions of the IF section are to amplify the down-converted IF signal from mixer, limit system noise and eliminate spurious signals introduced by mixer. It consists of a pre-amplifier, band-pass filter, and amplifier. The block diagram of IF section is shown in Fig. 7.

The bandpass filter is used to reduce the noise bandwidth and eliminate harmonic introduced by the mixer. The band-pass filter is designed to operate from 1.5 MHz to 35 MHz. In our design, the Butterworth filter is chosen because it provides a maximally flat passband and a monotonically increasing attenuation function in the stop band. The band-pass filter is implemented by a 8th order 1.5 MHz Butterworth high pass filter and 8th order 35 MHz Butterworth low pass filter.

The main functions of Data Acquisition Unit (DAU) are to digitize the video frequency signals, buffered the data, and route it to an on-board recorder. Fig. 8 shows the basic block diagram of our DAU. It consists of analog-to-digital converter (ADC), on board buffer, PCI interface and disk recorder. The ADC is capable of sampling two 12-

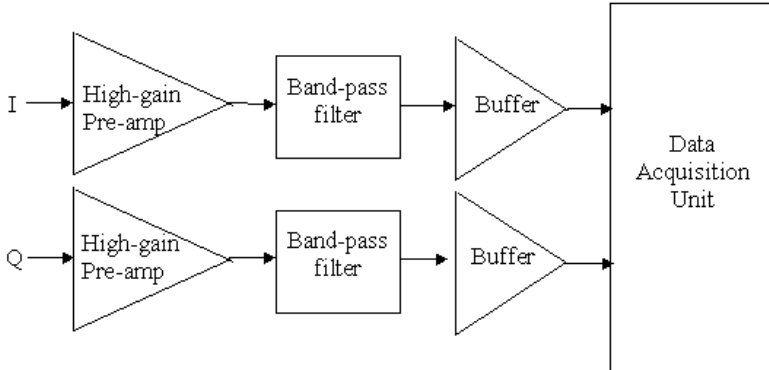


**Figure 7.** Block diagram of IF section.

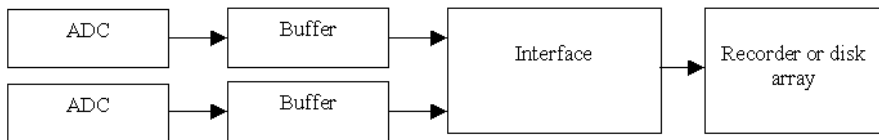


**Figure 8.** Data acquisition unit.

bits signals simultaneously with maximum sampling rate of 50 MS/s. The maximum transfer rate of the analogue input card to PC memory is 100 MB/s.

### 3. CALIBRATION AND VERIFICATION

The transmitter and the receiver of the airborne SAR system have been tested in laboratory and outdoor environment. Subsystem performance test, RF feedback calibration, and internal calibration are done in the laboratory to verify the performance of transmitter and receiver. Outdoor experiments are carried out to demonstrate the capability of the system in range detection and radar cross section (RCS) measurement. The detail descriptions of measurements are explained in the following sections.

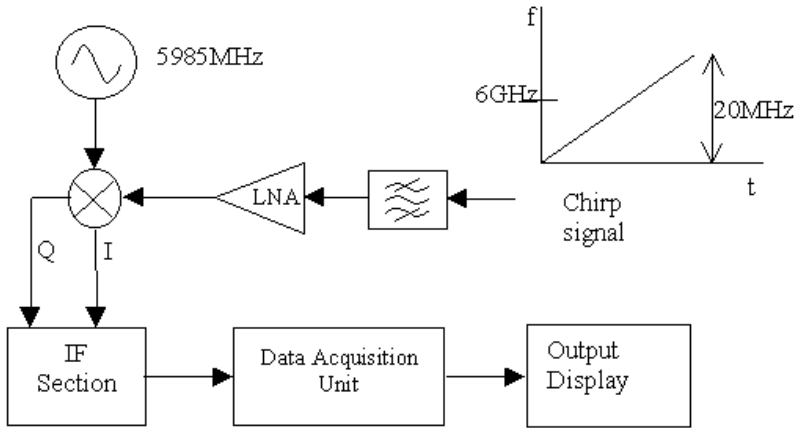


**Figure 9.** Measurement setup for receiver testing.

### 3.1. Subsystem Performance Test, RF Feedback Calibration and Internal Calibration

In subsystem performance test, both transmitter and receiver are tested. Transmitted power is monitored and signal waveform is verified. For the receiver chain, the noise floor is measured and the receiver gain is determined. A chirp waveform with center frequency of 6 GHz and 20 MHz bandwidth is generated by the chirp generator. The linearity of transmitted chirp is monitored and verified using the Agilent E4407B spectrum analyzer.

For receiver testing, a chirp signal with center frequency 6 GHz and 20 MHz bandwidth is injected into the front end of the receiver and the mixer LO input is fixed at 5.985 GHz. The configuration of the receiver testing is shown in Fig. 9. The down-converted signal will range from 5 to 25 MHz. Fig. 10 shows the digitized down-converted signal. The noise floor of the receiver system is approximately  $-70$  dB and the system gain is around 35 dB.

In RF feedback calibration, the transmitted signal is directly fed into the receiver. A delay line is used to delay the transmitted signal and a variable attenuator is used to accommodate the dynamic range of the receiver. Two different delay lines are used, 100 ns and 200 ns respectively. They are used to simulate a point target of 15 m and 30 m. Fig. 11 shows the measurement setup of the RF feedback calibration. The range of the point target is directly proportional to the intermediate frequency. After reconstructing the IF signal using FFT, the results are shown in Fig. 12 and Fig. 13. For each of the

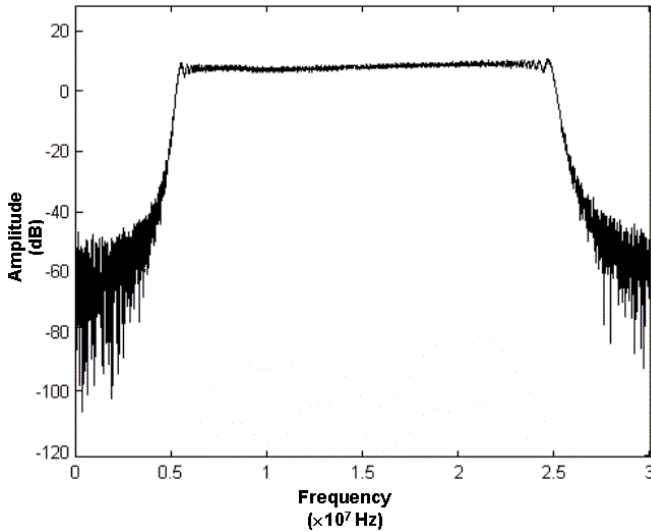


**Figure 10.** Output of analogue to digital converter (ADC) in frequency domain.

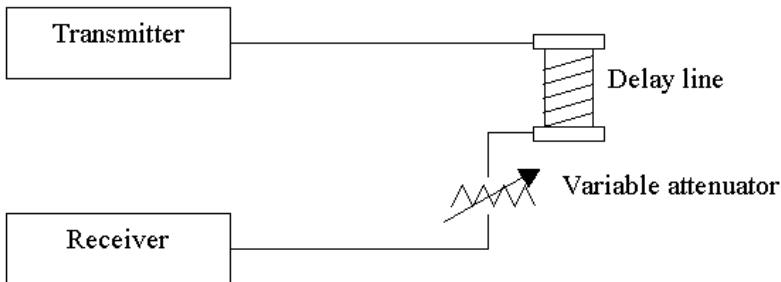


**Figure 11.** RF feedback calibration configuration.

delay line (100 ns and 200 ns), a peak return is observed at 15 m and 30 m, respectively.

The internal calibration is performed for the entire transmitter and receiver system. The configuration of the internal calibration is shown in Fig. 14. The antenna is replaced by a 100 ns delayed line and therefore simulates a point target with a range of 30 m. The chirp signal is transmitted via circulator by the transmitter, attenuated by the delay line, and reflected by the short circuit termination. The return signal is routed to receiver by the circulator. This signal is

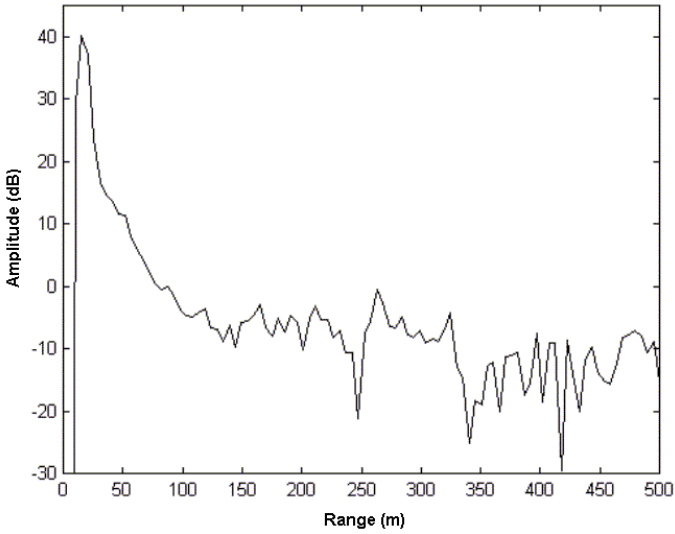


**Figure 12.** The measured power spectrum of 100 ns delay line.

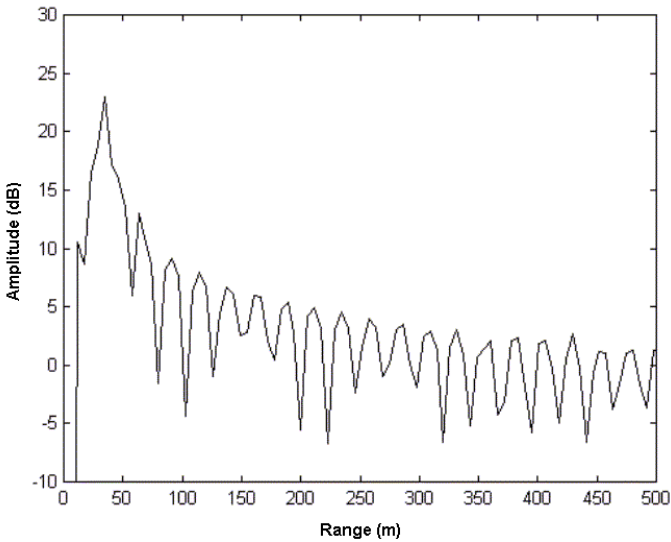


**Figure 13.** The measured power spectrum of 200 ns delay line.

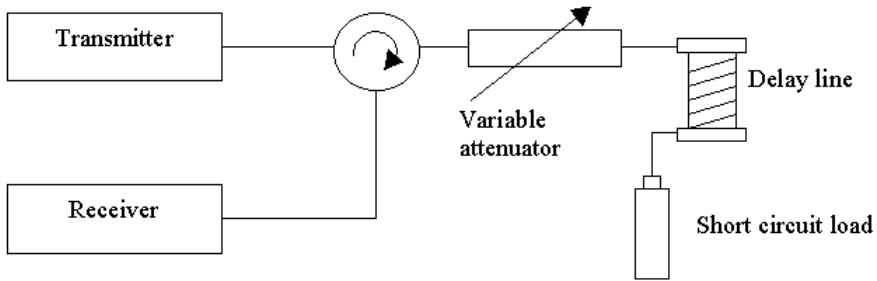


**Figure 14.** Measurement setup for internal calibration.

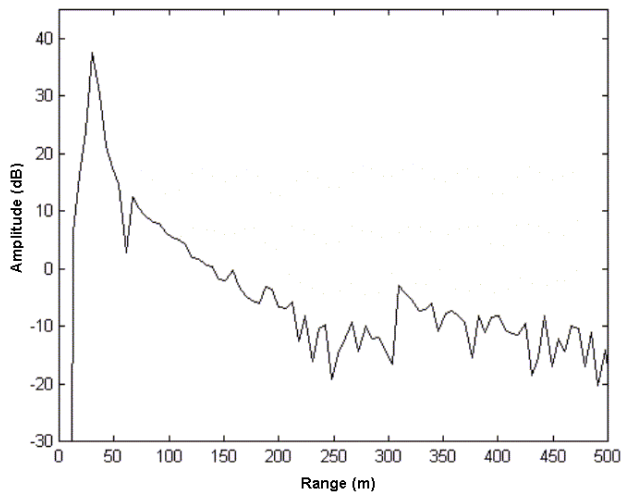


**Figure 15.** The measured power spectrum of 100 ns delay line.

down-converted, digitized and reconstructed using FFT (Fast Fourier Transform). The power spectral densities of measured return are given in Fig. 15. A peak return is observed at the target range of 30 m.

### 3.2. Field Measurement

Several field experiments have been conducted to verify the capability of the airborne SAR transmitter and receiver system. Point target calibration technique is utilized for external calibration. Three known artificial point targets, 12" conducting sphere, 4"  $\times$  8" dihedral corner reflector and 8" trihedral corner reflector are used in the field measurement. The targets have been carefully studied to evaluate the

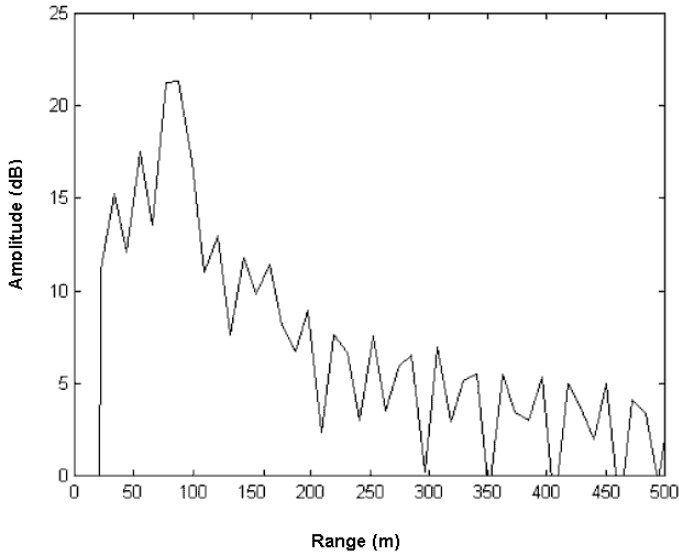


**Figure 16.** The measured power spectrum of 80 m range.

SAR system response. The field measurements are conducted in an empty car park, which is a low reflection outdoor environment.

For range detection the point target is put at different distance away from the antenna. The chirp waveform is transmitted by the antenna and the return echo is recorded and analyzed. Fig. 16 shows the power spectral densities of the measurement result when the target is placed 80 m away from the sensor. A peak return is observed at the range of 80 m. Thus the capability of range detection is verified. 12" conducting sphere, 4"  $\times$  8" dihedral corner reflector and 8" trihedral corner reflector are placed on a foam column, one after another for radar cross section (RCS) measurement. The point target is placed 50 m away from the antenna. Relative measurement has been performed in this experiment. The conducting sphere is used as the calibration standard in this experiment. The relative signals strength of trihedral corner reflector and dihedral corner reflector with respect to the conducting sphere are determined. Table 2 summarized the result of the RCS measurement. The measurement error for trihedral corner reflector is less than 0.5 dB, whereas an error of about 2 dB is observed for the dihedral corner reflector. The dihedral corner reflector has an extremely narrow beamwidth in the elevation plane. The measured RCS is lower than the theoretical value due to misalignment of the corner reflector.

**Table 2.** RCS measurement result.

	Measured RCS (dB)	Theoretical Value (dB)
Trihedral corner reflector	+4.32	+4.54
Dihedral corner reflector	+4.50	+6.30

#### 4. CONCLUSION

An experimental airborne SAR transmitter and receiver have been designed and constructed. Poor isolation of the circulator is overcome using a cancellation network. The leakage signal will be cancelled, hence the receiver LNA is prevented from saturation. A single antenna can therefore be used for transmitting and receiving the radar signal. A series of field measurements have been conducted to verify the capability of range detection and RCS measurement. The results showed good agreement with the theory. The results show the ability of the sensor to be used in geophysical remote sensing. The next step of work is to mount the SAR system onto an aircraft for actual field measurement.

#### REFERENCES

1. Curlander, J. C. and R. N. McDounough, *Synthetic Aperture Radar, Systems and Signal Processing*, John Wiley & Sons, New York, 1991.
2. Drinkwater, M. K., R. Kwok, and E. Rignot, "Synthetic aperture radar polarimetry of sea ice," *Proceeding of the 1990 International Geoscience and Remote Sensing Symposium*, Vol. 2, 1525–1528, 1990.
3. Lynne, G. L. and G. R. Taylor, "Geological assessment of SIR-B imagery of the Amadeus basin," *IEEE Trans. on Geosc. and Remote Sensing*, Vol. 24, No. 4, 575–581, 1986.
4. Hovland, H. A., J. A. Johannessen, and G. Digranes, "Slick detection in SAR images," *Proceeding of the 1994 International Geoscience and Remote Sensing Symposium*, 2038–2040, 1994.
5. Walker, B., G. Sander, M. Thompson, B. Burns, R. Fellerhoff, and D. Dubbert, "A high-resolution, four-band SAR Testbed with real-time image formation," *Proceeding of the 1986 International Geoscience and Remote Sensing Symposium*, 1881–1885, 1996.
6. Ulaby, F. T., R. K. Moore, and A. K. Fung, *Microwave Remote Sensing: Active and Passive*, I, Artech House, Norwood, 1981.

7. Knott, E. F., *Radar Cross Section Measurements*, Van Nostrand Reinhold, New York, 1993.

**Yee-Kit Chan** received his B.Eng. (Hons) in Electrical Engineering from the University of Malaya, in 1998 and M.Eng.Sc. in Electrical Engineering from the Multimedia University, in 2002. He is presently a lecturer with the Faculty of Engineering and Technology, Multimedia University. His research interests include microwave remote sensing, radar technology and RF circuit design. He is currently involved in the development of an airborne SAR system for remote sensing applications.

**Boon-Kuan Chung** graduated with a B.Eng. (Hons) in Electrical Engineering from the University of Malaya in 1992. He worked in the Design Department of Sony Electronics in Penang, Malaysia from 1992 to 1995. He then returned to the University of Malaya to undertake a research project and obtained his M.Eng.Sc. degree in Electrical Engineering in 1997. He obtained his Ph.D. in Microwave Engineering from Multimedia University in 2003. He is currently a senior lecturer at Multimedia University. His research interests include microwave theory and techniques, radar, wireless communication systems, antenna design, remote sensing, electromagnetic compatibility, and electronic instrumentation and measurements.

**Hean-Teik Chuah** obtained his B.Eng., M.Eng.Sc., and Ph.D., all in electrical engineering, from the University of Malaya. He is currently the Dean of Faculty of Engineering, Multimedia University. Chuah was the recipient of the inaugural Young Engineer Award by the Institution of Engineers, Malaysia in 1991, the 1995 National Young Scientist Award (Industrial Sector) by the Malaysian Ministry of Science, Technology and the Environment, and the recipient of 1999 Malaysia Toray Science and Technology Award. His research interest are in applied electromagnetic, microwave remote sensing, and device physics.